

Sequential Cross Correlation: A Robust Technique to Detect Brain Activation in fMRI

X. Xu¹, S. Lai¹

¹Department of Radiology, Thomas Jefferson University, Philadelphia, PA, United States

Introduction

Sequential test is generally designed to detect presence of a signal at an earlier stage than fixed length test when data arrives sequentially [1-3]. One often overlooked feature of sequential test is that it can detect signal more robustly than fixed length test [4]. Herein, in the framework of sequential test, we present a novel method, dubbed sequential cross correlation (SCC), to detect brain activation in fMRI. SCC calculates and stores cross correlation coefficients between a reference waveform (RW) and time course (TC) as more data are sequentially collected. Compared with standard cross correlation (CC) method [5], which is a fixed length test and does not track temporal behavior of the data [6] and thus may be prone to errors caused by outliers in the data, SCC is able to extract the intrinsic temporal structure of the data and as such can improve brain activation detection. SCC can be applied both on-line for real time fMRI applications, and off-line to post-process fMRI data. The same concept of sequential test can also be applied to other statistical methods (i.e., student t-test, Z score, etc).

Materials and Method

Given two vectors, a RW and a TC, both of length N , SCC generates a vector (**SC**) of cross correlation coefficients (CCC) of the same length N . At each temporal point n ($=2,3,\dots,N$), **SC**(n) is computed as the CCC between two sub vectors **RW**($1:n$) and **TC**($1:n$) where **RW**($1:n$) stands for the first n elements of RW and similar meaning stands for **TC**($1:n$). **SC**(1) is initialized to zero. Mathematically, **SC**(n) is given by

$$\mathbf{SC}(n) = \text{cross correlation between RW}(1:n) \text{ and TC}(1:n), \text{ for } n=2,3,\dots,N.$$

Therefore, **SC** intrinsically tracks temporal behavior of CCC as new data arrives. Note that the last element, **SC**(N), equals the CCC given by conventional CC using full length of data. **SC** can be computed effectively using recursive implementation. As shown by examples below, for a highly activated pixel, corresponding **SC** has 1) more large absolute values and 2) relatively smooth pattern. On the other hand, **SC** of a non-activated pixel has 1) relatively small values and 2) more random pattern. Based on this observation, **SC** can be analyzed to produce better results in detection. In this work, SCC was designed by exploiting the above first feature to distinguish activated pixels from non-activated ones. Given a preset threshold $a > 0$ and pixel position $[i,j]$, final output P_{ij} was computed as

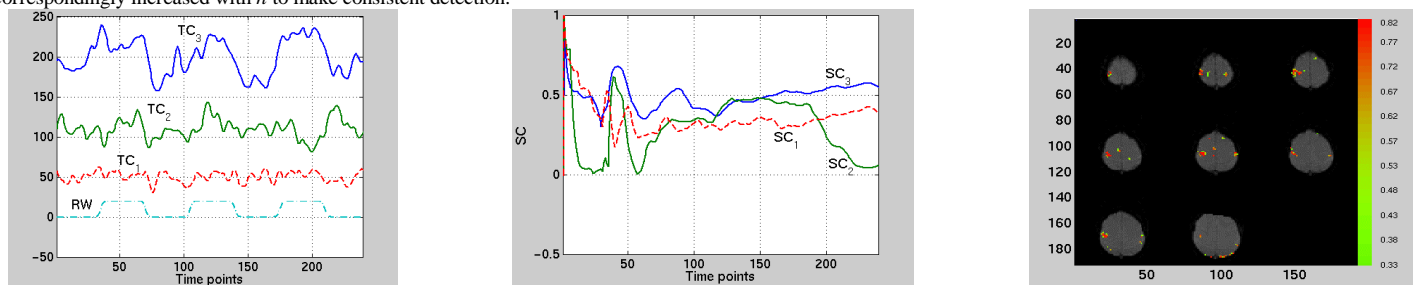
$$P_{ij} = \text{total number of } \mathbf{SC}_{ij}(n) \text{ such that } \mathbf{SC}_{ij}(n) > a, \text{ for } n=1,2,3,\dots,N.$$

P is then thresholded at $M > 0$ to generate the final output.

Finger tapping activation data were obtained on a clinical whole-body 1.5-T MRI scanner (Magnetom Vision, Siemens Medical Systems, Erlangen, Germany) equipped with a standard circularly polarized radio-frequency head coil. Stimulus consisted of 3 cycles of "30s OFF/30s ON" bilateral finger tapping followed by 30s of OFF period. A gradient echo EPI sequence was used ($TR/TE/\alpha = 0.88s/40ms/90^\circ$) in the experiment.

Results

SCC was applied on bilateral finger tapping fMRI data to assess its performance. For the purpose of illustration, three representative TC's were chosen. Below, the left figure shows a RW and three TC's, where TC1 is a non-activated pixel time course and TC2 and TC3 are activated pixel time course. (Note that the vertical axis is not labeled because constants have been added to RW and TC's to separate them in the figure for visual appreciation. In our case, adding constants to waveforms does not change the CCC since in calculation waveforms were demeaned at first.) The central figure plots the **SC**1 of TC1, dash line; and **SC**2 of TC2 and **SC**3 of TC3, solid line. By comparing **SC**1 with **SC**2 (**SC**3), it is noted that they do differ in the two aspects aforementioned. Note the irregular increase of **SC**1 at the end, if threshold a is set at 0.35, conventional CC would make a false alarm about TC1. At the same threshold conventional CC would reject TC2 as an activated time course. On the other hand, SCC can correctly decide TC1 as nonactivated and TC2 as activated because, though **SC**1 increases at the end, a large number of it is lower than the threshold, and vice versa for **SC**2. For strongly activated signal such as TC3, both conventional CC and SCC make the correct detection. The strength of SCC lies in the fact it can detect some activated pixels missed by CC. The right figure shows the activation map obtained by SCC with a preset threshold a of 0.35, M of 85 and cluster size of 4. It detects 155 activated pixels. Using the same a and cluster size, conventional CC detects 102 activated pixels (image is not shown). In real time processing, as current time point n increments, M is correspondingly increased with n to make consistent detection.



Conclusions

Instead of relying on the CCC of full length data as conventional CC does, SCC takes into consideration of temporal behavior of the data and, thus, is able to maintain sensitivity to changes in the data. SCC was used to post-process fMRI data in this work. With minor modification, SCC can be generated to process fMRI data in real time. Work is in progress in this lab to exploit more distinct features between **SC**1 and **SC**2, with our aim being to develop a framework for choosing thresholds a (i.e., CCC threshold) and M (i.e., corresponding number of time points in SC that have CCC $> a$).

References

- [1] Helstrom CW. Elements of Signal Detection and Estimation. Prentice-Hall, 1994.
- [2] Wald A. Sequential Analysis. Wiley, 1947.
- [3] Siegmund D. Sequential Analysis: Tests and Confidence Intervals. Springer-Verlag, 1985.
- [4] Xu X, et al. IEEE Trans Geosci. & Rem. Sens. 2002;40:4:963-976.
- [5] Bandettini PA, et al. Magn Reson Med 1993;30:161-173.
- [6] McKeown MJ, et al. Human Brain Mapping 1998;6:160-188.